

# GENERATION OF GEV PHOTONS FROM X-RAY FREE ELECTRON LASER OSCILLATORS

R. Hajima\*, M. Fujiwara<sup>1</sup>

National Institutes for Quantum and Radiological Science and Technology (QST),  
Tokai, Ibaraki, 3191106, Japan

<sup>1</sup>also at Osaka University, Mihogaoka 10-1, Ibaraki, Osaka 5670047, Japan

## Abstract

We propose generation of narrow-bandwidth GeV photons, gamma-rays, via Compton scattering of hard X-ray photons in X-ray free-electron laser oscillators [1]. The gamma-rays have a narrow-bandwidth spectrum with a sharp peak, ~0.1% (FWHM), due to the nature of Compton scattering in relativistic regime. Such gamma-rays will be a unique probe for studying hadron physics. In this paper, we discuss design and performance of the gamma-ray source.

## INTRODUCTION

Generation of high-energy photons via collision of relativistic electrons and laser photons is known as laser Compton scattering (LCS). LCS photon sources have been developed and used in a wide range of photon energies from keV to GeV, since LCS photons are energy tunable according to electron beam energy, laser wavelength and collision geometry [2]. Typical applications of LCS photon sources are imaging for medical purposes in keV [3], science of photonuclear reaction and its utilization for nuclear industry in MeV [4, 5], and hadron physics in GeV [6].

LCS photon sources in keV and MeV energies are recognized as Thomson scattering in the electron rest frame, because a laser photon energy in the rest frame is much smaller than the electron rest mass. Scattering, however, becomes Compton regime as a laser photon energy at the rest frame is comparable to or larger than the electron rest mass.

For the head-on collision, the maximum energy of scattered photon and the energy differential cross-section are given as [7]

$$\epsilon_2^{max} = \frac{4\gamma_e^2 \epsilon_1}{1 + 4\gamma_e \epsilon_1}, \quad (1)$$

$$\frac{d\sigma_c}{d\epsilon_2} = \frac{\pi r_0^2}{2} \frac{1}{\gamma_e^2 \epsilon_1} \left[ \frac{1}{4\gamma_e^2 \epsilon_1^2} \left( \frac{\epsilon_2}{\gamma_e - \epsilon_2} \right)^2 - \frac{1}{\gamma_e \epsilon_1} \left( \frac{\epsilon_2}{\gamma_e - \epsilon_2} \right) + \frac{\gamma_e - \epsilon_2}{\gamma_e} + \frac{\gamma_e}{\gamma_e - \epsilon_2} \right], \quad (2)$$

where  $\sigma_c$  is the cross-section of Compton scattering,  $r_0$  is the classical electron radius,  $\gamma_e = E_e/mc^2$ ,  $\epsilon_1 = E_1/mc^2$  and  $\epsilon_2 = E_2/mc^2$  are the electron, incident and scattered photon energies normalized by the electron rest mass, respectively.

We plot energy differential cross section for Thomson and Compton regimes in Fig.1, where we assumed electron

energy of 7 GeV and laser photon energies of 1.2 eV and 12 keV. We see that generation of a narrow-band  $\gamma$ -ray beam is possible via Compton scattering of hard X-ray photons and relativistic electrons.

In this paper, we propose a scheme to realize such devices by using X-ray free-electron laser oscillator (XFELO) and discuss design and performance of such  $\gamma$ -ray source, XFELO- $\gamma$ .

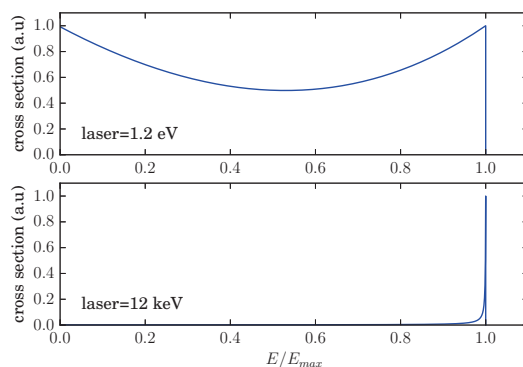


Figure 1: Energy-differential cross-section of laser photons scattered with 7 GeV electrons: laser photon energies of 1.2 eV (Thomson regime) and 12 keV (Compton regime).

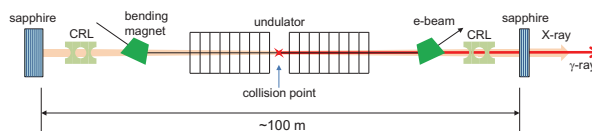


Figure 2: Schematic views of an X-ray FEL Oscillator.

## DESIGN PARAMETERS OF XFEL0- $\gamma$

We consider an XFEL0- $\gamma$  shown in Fig. 2. The X-ray oscillator utilizes two normal-incidence flat sapphire ( $\alpha - \text{Al}_2\text{O}_3$ ) crystals in combination with compound refractive lenses (CRL). Parameters of XFEL0 are summarized in Table 1. We assume parameters similar to Refs. [8,9] and the electron beam parameters suggested in Ref. [10]: electron energy is chosen at  $E_e = 7$  GeV to produce an X-ray beam of 1 Å and the repetition of XFEL0 is chosen at 3 MHz so that an electron bunch has a collision with a backward X-ray pulse at the center of a 100-m-long cavity.

\* email address: hajima.ryoichi@qst.go.jp

Table 1: Parameters of the XFELO for XFELO- $\gamma$ 

Electron beam	
Energy ( $E_e$ )	7 GeV
Bunch charge ( $Q$ )	40 pC
rms energy spread ( $\sigma_{\Delta E}$ )	1.4 MeV
Normalized rms emittance ( $\varepsilon_n$ )	0.082 mm-mrad
rms bunch length ( $\tau_e$ )	2 ps
Bunch repetition ( $f$ )	3 MHz
Undulator	
Undulator parameter ( $K$ )	1.414
Pitch ( $\lambda_u$ )	1.88 cm
The number of periods ( $N_u$ )	3000
FEL	
Wavelength ( $\lambda$ )	1 Å
Energy ( $E_1$ )	12.3 keV
Cavity length ( $L_c$ )	100 m
Small signal gain	50%
Round trip loss	17%
Out couple	4%
rms pulse length ( $\tau_X$ )	0.85 ps
rms energy spread ( $\sigma_{\Delta E_1}$ )	2.3 meV
Collision parameters	
Beta function ( $\beta^*$ )	10 m
Rayleigh length ( $Z_R$ )	10 m
Electron beam rms size ( $\sigma_e$ )	7.7 $\mu\text{m}$
Electron beam rms divergence ( $\sigma'_e$ )	0.77 $\mu\text{rad}$
X-ray beam rms size ( $\sigma_X$ )	8.9 $\mu\text{m}$
X-ray beam rms divergence ( $\sigma'_X$ )	0.89 $\mu\text{rad}$
The number of electrons ( $N_e$ )	$2.5 \times 10^8$
The number of X-ray photons ( $N_X$ )	$2.0 \times 10^{10}$

## PERFORMANCE OF XFELO- $\gamma$

In generation of LCS beams for keV and MeV photon energies, quasi-monochromatic photon beams are obtained with a collimator to restrict scattering angle of photons reaching to an experimental station. Energy bandwidth of a LCS beams after a collimator is primarily determined by opening angle of the collimator and has additional spectral dilution due to inhomogeneous effects such as divergence and energy spread of electron and laser beams at the collision [11].

On the other hand, generation of narrow-band  $\gamma$ -rays from the XFELO- $\gamma$  is attributed to the nature of Compton scattering, not to the beam collimation. Theoretical analysis revealed that the spectral dilution in XFELO- $\gamma$  is dominated by electron energy spread and other inhomogeneous effects can be neglected [1].

A simulation code CAIN [12] is adopted to evaluate the XFELO- $\gamma$  performance, flux, spectrum, with the effects of energy spread of electrons and finite divergence of electron and X-ray beams at the collision. Note that the CAIN simulations do not include the energy spread of X-ray photons, but this effect is negligibly small.

The electron beam energy spread at the collision point should be evaluated by taking into account the FEL inter-

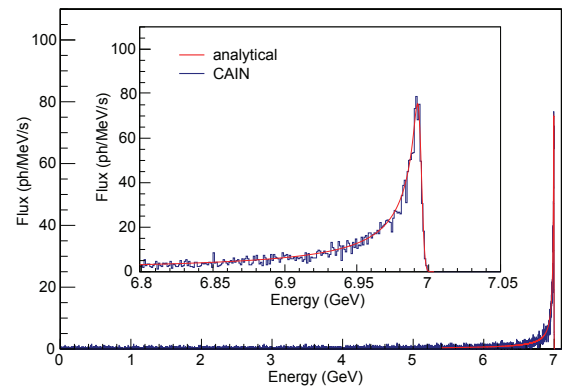


Figure 3:  $\gamma$ -ray spectra of the two-mirror 7-GeV XFELO- $\gamma$  calculated by analytical formula with electron energy spread (red) and numerical simulation by CAIN (blue).

Table 2: Calculated Performance of the XFELO- $\gamma$  with Parameters Listed in Table 1.

Repetition	3 MHz
Peak energy	6.9922 GeV
Bandwidth (FWHM)	12 MeV
Flux (100% BW)	4900 ph/s
Flux (1% BW)	1700 ph/s
Flux (0.1% BW)	460 ph/s

action. For an undulator with a period of  $N_u$ , the energy spread induced by the FEL interaction is  $(\sigma_E/E_e)_{FEL} \sim 12/(4\pi N_u)$  at the end of undulator [13]. We assume an energy spread as a half of the aforementioned value at the center of undulator. For the XFELO- $\gamma$  with the parameter listed in Table 1, the electron beam at the center of undulator has an energy spread of  $\sigma_E = 1.8$  MeV including the contribution of FEL interaction.

Figure 3 shows the  $\gamma$ -ray spectrum obtained from the numerical simulation together with an analytically calculated spectrum for the XFELO- $\gamma$ . The analytical curve correspond to a spectrum calculated using Eq.(2) convoluted by electron energy spread,  $\sigma_E = 1.8$  MeV. The numerical result is in good agreement with the analytical one. This agreement also supports the fact that the  $\gamma$ -ray bandwidth is insensitive to divergence of electrons and laser photons at the collision.

The numerically calculated performance of the XFELO- $\gamma$  is summarized in Table 2.

## DISCUSSION AND OUTLOOK

We discuss the energy tunability and the enhancement of the  $\gamma$ -ray flux from the design with parameters listed in Table 1. The  $\gamma$ -ray peak energy in an XFELO- $\gamma$  is insensitive to the X-ray photon energy, but is determined by the electron energy. Several design studies of XFELO for hard X-ray generation have been carried out, where the electron energy ranges from 3.5 GeV [14] to 10 GeV [8], i.e.  $\gamma$ -ray peak energy can be chosen at a specific energy between 3.5 and 10 GeV. The  $\gamma$ -ray peak energy is further tunable con-

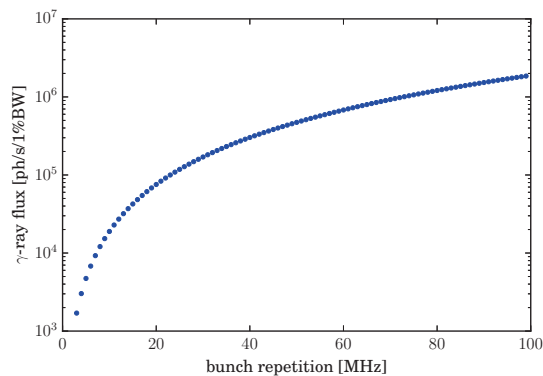


Figure 4:  $\gamma$ -ray flux in the XFELO- $\gamma$  as a function of bunch repetition from 3 MHz to 100 MHz.

tinuously from the specific energy with varying the electron beam energy and undulator gap as far as FEL lasing is obtained with given undulator and crystal mirrors. According to the FEL physics, variation of the undulator parameter from  $K = 1.414$  to  $K = 0.930$  results in the variation of the electron beam energy from 7 GeV to 5.93 GeV to keep the FEL wavelength at 1 Å. The variation of the electron energy, however, introduces a FEL gain reduction of 30% from the design at 7 GeV. Available tuning range of the  $\gamma$ -ray peak energy by varying the electron energy depends on the parameters of the XFELO to determine FEL gain margin over the oscillator loss.

Since there is a feasibility for XFELO to be operated with the repetition of 1-100 MHz as suggested in Ref. [8], the  $\gamma$ -ray flux of XFELO- $\gamma$  is increased with increasing the electron beam repetition. The enhancement factor for the XFELO- $\gamma$  is expressed to be  $2\eta L_c L_s / L_b^2$ , where  $L_c$  is the cavity length,  $L_b$  is the electron bunch interval,  $L_s$  is the length of interaction region between two bending magnets,  $\eta^{-1} = 1 + (L_s / \sqrt{12} Z_R)^2$  is a correction factor for the variation of the collision spot size along the interaction region. Figure 4 shows  $\gamma$ -ray flux as a function of bunch repetition from 3 MHz to 100 MHz.

The  $\gamma$ -ray flux is also increased with increasing the intracavity X-ray photons using a smaller out-coupling of the X-ray oscillator. Detailed analysis of thermal issues on crystal mirrors is necessary in a practical design of XFELO- $\gamma$ , because the repetition of electron bunch and the out-coupling of oscillator are both limited by thermal deformation of crystal mirrors. We note that the number of  $\gamma$ -ray photons generated from an electron bunch is much smaller than the number of electrons in a bunch even with the multiple collisions. Thus, the X-ray lasing is not affected by Compton scattering.

For  $\gamma$ -ray application experiments, it is possible to determine  $\gamma$  photon energy by measuring the energy of recoil electron with a tagging counter, which may be accompanied by a beam-line collimator to eliminate the low-energy  $\gamma$  photons at the experimental area. The energy measurement of recoiled electrons in an XFELO- $\gamma$  can be conducted with chicane magnets or a small bending magnet before the main

magnet to deflect the 7-GeV electrons. Since the most of  $\gamma$ -ray photons are concentrated around the peak energy, we only need to measure low-energy electrons, below 100 MeV for example. The accuracy of photon energy measurement is restricted by electron beam energy spread at the collision, 1.8 MeV (rms) for the XFELO- $\gamma$ .

We also discussed alternative layout of XFELO- $\gamma$  with a four-mirror oscillator and generation of circularly polarized  $\gamma$ -rays from a spin polarized electron beam elsewhere [1].

The XFELO- $\gamma$  will open a new opportunity for studying the charmed quark ( $c$ -quark) production dynamics from proton and neutron which mainly consist of  $u$ - and  $d$ -quarks. In the past, the production of  $\phi$ ,  $\Lambda$  and  $\Sigma$  particles including strangeness quarks has been studied at the Jefferson Laboratory and at the SPring-8 [15]. In future, new types of experiments with an XFELO- $\gamma$  will be realized to produce, i.e., the  $J/\Psi$  meson and charmed baryons from the  $u$ - and  $d$ -quark medium [16].

## REFERENCES

- [1] R. Hajima and M. Fujiwara, Phys. Rev. Accel. Beams, **19**, 020702 (2016).
- [2] G.A. Krafft and G. Priebe, Rev. Accl. Sci. Tech. **03**, 147 (2010).
- [3] K. Achterhold, M. Bech, S. Schleede, G. Potdevin, R. Ruth, R. Loewen, F. Pfeiffer, Sci. Rep. **3**, 1313 (2013).
- [4] H.R. Weller *et al.*, Progress in Particle and Nuclear Physics, **62**, 257 (2009).
- [5] R. Hajima *et al.*, Eur. Phys. J. Special Topics **223**, 1229 (2014).
- [6] M. Fujiwara, Progress in Particle and Nuclear Physics, **50**, 487-497 (2003).
- [7] F.R. Arutyunian and V.A. Tumanian, Phys. Lett. **4**, 176 (1963).
- [8] Kwang-Je Kim, Yuri Shvyd'ko and Sven Reiche, Phys. Rev. Lett. **100**, 244802 (2008).
- [9] Kwang-Je Kim and Yuri Shvyd'ko, Phys. Rev. ST-AB **12**, 030703 (2009).
- [10] I.V. Bazarov and C.K. Sinclair, Phys. Rev. ST-AB **8**, 034202 (2005).
- [11] V. Petrillo *et al.*, Nucl. Instr. Meth. A **693**, 109 (2012).
- [12] CAIN ver. 2.42; P. Chen, G. Horton-Smith, T. Ohgaki, A.W. Weidemann, K. Yokoya, Nucl. Instr. Meth. A **355**, 107 (1995).
- [13] E.L. Saldin, E.A. Schneidmiller, M.V. Yurkov, *The Physics of Free Electron Lasers* (Springer-Verlag Berlin Heidelberg, 1999).
- [14] Jinhua Dai, Haixiao Deng and Zhimin Dai, Phys. Rev. Lett. **108**, 034802 (2012).
- [15] T. Nakano *et al.*, Nucl. Phys. A **684**, 71c-79c (2001).
- [16] K.A. Olive *et al.* (Particle Data Group), Chin. Phys. C **38**, 090001 (2014).